Chinese Chemical Letters 33 (2022) 243–246

Contents lists available at ScienceDirect

Chinese Chemical Letters

journal homepage: www.elsevier.com/locate/cclet

A micro-wave strategy for synthesizing room temperature phosphorescent materials

Ru Liang[a], Lijun Huo[a], Ao Yu[a], Jinjing Wang[a], Chunman Jia[a,*], Jianwei Li[a,b,**]

[a] Hainan Provincial Key Laboratory of Fine Chemicals, College of Chemical Engineering and Technology, Hainan University, Haikou 570228, China
[b] MediCity Research Laboratory, University of Turku, Tykistökatu 6, Turku 20520, Finland

ARTICLE INFO

Article history:
Received 23 March 2021
Revised 20 May 2021
Accepted 21 May 2021
Available online 27 May 2021

Keywords:
Carbon dots
Room temperature phosphorescence
Boron doping
Afterglow
Microwave method

ABSTRACT

Room temperature phosphorescent (RTP) materials have a variety of applications ranging from bio-imaging, optoelectronic devices to information security protection. However, the preparation procedures for these materials are always tedious and time-consuming. Here, we report a micro-wave approach to prepare RTP carbon dots (CDs) in only 8 min. The micro-wave promoted the carbon and boron bond formation using natural compounds glucose and boric acids. This result has been confirmed using TEM, FTIR, XPS and XRD measurements. The C-B hetero atomized material presented a long afterglow property. With the irradiation with UV light, we observed an eight-second RTP by naked eyes after the lamp was turned off, and the phosphorescence lifetime was 487 ms. This excellent performance was mainly due to the formation of B-C bonds that promoted the intersystem crossings (ISC) and non-radiation transition of triplet states. Moreover, the glass state of the materials also helped to stabilize the triplet states of B-CDs and made its non-irradiation inactivated, which resulted in the characteristics of yellow green RTP. These results have demonstrated that micro-wave is a convenient and effective strategy to make hetero atomized RTP material, providing new possibilities for their industrial productions.

Room temperature phosphorescent (RTP) materials have a wide range of potential application in the fields of bio-imaging, optoelectronic devices, and information security protection, and have received extensive attention from scholars in recent years [1–12]. At present, the most effective RTP materials are metal doped inorganics and organometallic compounds [13–18]. As these materials usually contain precious metals, their synthesis cost is high, and they have cytotoxicity and poor stability. In recent years, as a new type of zero-dimensional carbon nanomaterials, carbon dots (CDs) can get over these disadvantages of RTP materials containing metals and have unique optical properties, being a rising star of metal-free RTP materials [19–27]. Generally, two strategies have been applied for a better RTP performance of CDs. CDs can be embedded as guests in polyvinyl alcohol [28], aluminum sulphate [29], zeolite [30], silicon dioxide [31], melamine [32], boric acid [33], and alum [34] or other different matrices [35,36]. The doping of these matrices can stabilize the emission of triplet states, effectively reduce the energy level difference between singlet and triplet states (ΔEst) and promote intersystem crossings (ISC). The synthesis of these materials generally needs two steps. CDs are first obtained using high-temperature and high-pressure experimental conditions in more than 10 h, and then they are introduced in the matrix to obtain a material with RTP performance. The above-mentioned preparation process is cumbersome and thereby is not conducive to industrialized mass production. The other strategy is to introduce N [37], P [38], F [39], B [40] and other heteroatoms in CDs [41], as they can promote ISC and reduce radiation jump of the triplet state.

In the choice of carbon sources, researchers mostly choose alcohols [42] and amines [39] as pure organic raw materials for the synthesis. Unfortunately, these starting materials are harmful for the environment and difficult to be widely used. In response to the drawbacks of the above studies, here we report a simple and rapid method to synthesize RTP CDs doped by boron atoms (B-CDs) in only 8 min using glucose as the environmentally friendly carbon source. The as prepared B-CDs emitted a long persistence of 8 s after being irradiated by an ultraviolet lamp and had a small ΔEst which could effectively complete the ISC.

In general, the B-CDs were prepared as following: Boric acid (1.5 g) was first dissolved in 30 mL of deionized water, in which

* Corresponding author.
** Corresponding author at: Hainan Provincial Key Laboratory of Fine Chemicals, College of Chemical Engineering and Technology, Hainan University, Haikou 570228, China.
E-mail addresses: jiachunman@hainanu.edu.cn (C. Jia), jianwei.li@utu.fi (J. Li).

https://doi.org/10.1016/j.cclet.2021.05.046
1001-8417/

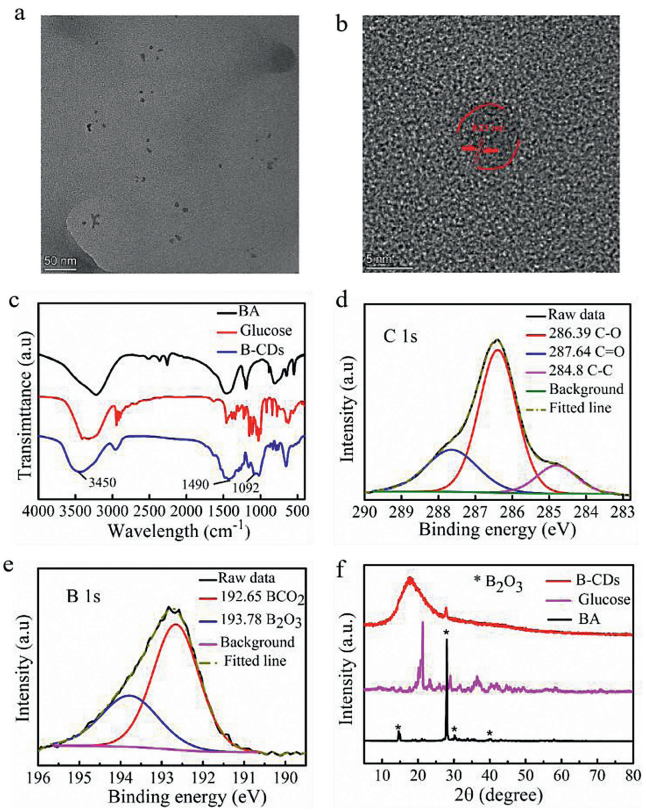

Fig. 1. (a) TEM analysis; (b) HR-TEM analysis of B-CDs; (c) FTIR spectra of boric acid, glucose and B-CDs; (d) C 1s and (e) B 1s spectrum of B-CDs using XPS of B-CDs; (f) XRD of B-CDs material, boric acid and glucose.

a certain amount of glucose was added. The resulting solution was heated using a household microwave oven for 8 min (640 W) and then cooled down to room temperature. The final B-CDs was obtained by lyophilizing the reaction solution. After we obtained the materials, their morphology was first studied using transmission electron microscopy (TEM). As shown in Fig. 1a, the materials were nanoparticles with similar sizes. Their average particle size was about 3.4 nm (Fig. S1 in Supporting information). High-resolution transmission electron microscopy (HR-TEM) analysis suggested that the materials were composed of amorphous and crystalline structures with a lattice spacing of 0.21 nm (Fig. 1b) which was consistent with the (100) facet of graphite [43–46].

To verify whether CDs were hetero atomized with boron, we analysed the materials using Fourier transform infrared spectroscopy (FTIR), X-ray photoelectron spectroscopy (XPS) and X-ray diffraction (XRD). The FTIR spectra of B-CDs materials showed main characteristic peaks at 3450 cm^{-1}, 1490 cm^{-1} and 1092 cm^{-1}. By comparing the characteristic peaks of samples prepared from only glucose and only boronic acids, the peaks at 1490 cm^{-1} and 3450 cm^{-1} should be attributed to the stretching vibration of B-O bond and O-H bond, respectively. The peak at 1092 cm^{-1} only appeared in the B-CDs materials, which was assigned to the stretching vibration of C-B bond (Fig. 1c) [47], suggesting that the boron atom was successfully introduced into the glucose. To confirm this result, the B-CDs materials were further investigated using X-ray photoelectron spectroscopy (XPS). The C 1s spectrum of the B-CDs material displayed peaks at 284.8 eV, 286.4 eV and 287.6 eV due to different carbon species sp^2 C, C-O and C=O, respectively (Fig. 1d). The analysis of B 1s spectrum revealed two peaks at 193.8 eV and 192.6 eV which were assigned to B_2O_3 and BCO_2 [48], respectively (Fig. 1e), indicating the formation of B-C bond. XRD analysis of the B-CDs showed that the material should be in an amorphous glass state (Fig. 1f). Interestingly, a distinct peak was observed at 27.8 which was also appeared in the sample prepared from only boric acid, suggesting that B atom was introduced to glucose. All together, glucose and boric acid reacted after microwave irradiation to form a B-C covalent bond in the B-CDs nanomaterial. This would play an essential role in improving the RTP performance [49].

Encouraged by the successful synthesis of CDs, we continued to study its RTP property. The materials were first irradiated by UV light at 365 nm. After the lamp was turned off, the material emitted a bright yellow-green and a long-lasting phosphorescence that lasted for 8 s (Fig. 2a). To elucidate the delayed phosphorescence phenomenon, we investigated the fluorescent and phosphorescent spectra of the material. As shown in Fig. 2b, as the excitation wavelength increased from 360 nm to 440 nm, the fluorescent emission wavelength increased in general, and a red shift occurred. The highest emission intensity was observed when the material was excited at 420 nm. It is important to point out that, the phosphorescence emission was different. Upon the excitation from 400 nm to 480 nm, the persistence emission peak was concentrated at 530 nm without distinct shift (Fig. 2c). The UV absorption spectrum of the B-CDs material in Fig. 2d shows that two peaks at 275 nm and 420 nm, which belong to the π-π^* transition of C=C bonds and the n-π^* transition of C=O bonds, respectively [43]. In addition, we also tested the lifetime of the persistence emission at 530 nm of the B-CDs material under the excitation at 365 nm (Fig. 2e). According to the fitting formula of the three-exponential function: $\tau_{avg} = \Sigma\alpha_i\tau_i^2/\Sigma\alpha_i\tau_i$, the average lifetime was determined as 487 ms, which proves that the persistence emission came from phosphorescence. In addition, when the B-CDs material was investigated under the temperature rising from 100 K to 400 K, the intensity of the persistence emission was decreased (Fig. 2f). That's due to the typical feature of phosphorescence radiation deactivation induced by temperature increase. These results further confirmed that the afterglow of the material was phosphorescent. The quantum efficiency of phosphorescence is 14.5%.

To further study the RTP property of the material, we measured the phosphorescence emission intensity of B-CDs prepared from boric acid (3 g) and various amounts X of glucose (X = 0, 2.5, 3, 4, 5 g). The materials were named as B-CDs_x and X was equalled to the amounts of glucose used. As shown in Fig. 3a, the phosphorescence emission intensity of materials made from only boric acid B-CDs_0 was very weak while the B-$CDs_{2.5}$ material had the strongest phosphorescence emission intensity. This should be attributed to the formation of B-C bonds. Then, the B-C bonds of the B-$CDs_{(2.5,\ 3,\ 4,\ 5)}$ were checked by using FTIR (Fig. 3b). The B-$CDs_{2.5}$ showed the strongest characteristic peak of B-C bonds at 1092 cm^{-1}, but the peak trended to be weakened as the increase in the proportion of glucose. These results further confirmed that the formation of the B-C bond affected the life and RTP performance of the material. In the XRD pattern of Fig. 3c, compared with the other three ratios of glucose, B-$CDs_{2.5}$ showed a distinct enhancement at 27.8, which is a characteristic peak of boric acid, corresponding to the (002) crystal plane of graphene. The introduction of boron atoms changed the crystal form of the material, and the introduction of the special crystal form of boric acid into B-CDs played an important role in improving the performance of the material. In addition, in Fig. 3d, the lifespan of B-$CDs_{2.5}$ was the longest, reaching 487 ms, and the phosphorescence lifetime of B-CDs_4 was the shortest, 217 ms. This indicated that the strength of the boron-carbon bond formed by the combination of different levels of glucose and boric acid affected the performance of RTP in B-CDs. To confirm that the formation of boron-carbon bond was significant to the optical property of the material, we did a control experiment by preparing a material from only glucose. No fluorescence and phosphorescence were observed (Figs. 3e and f).

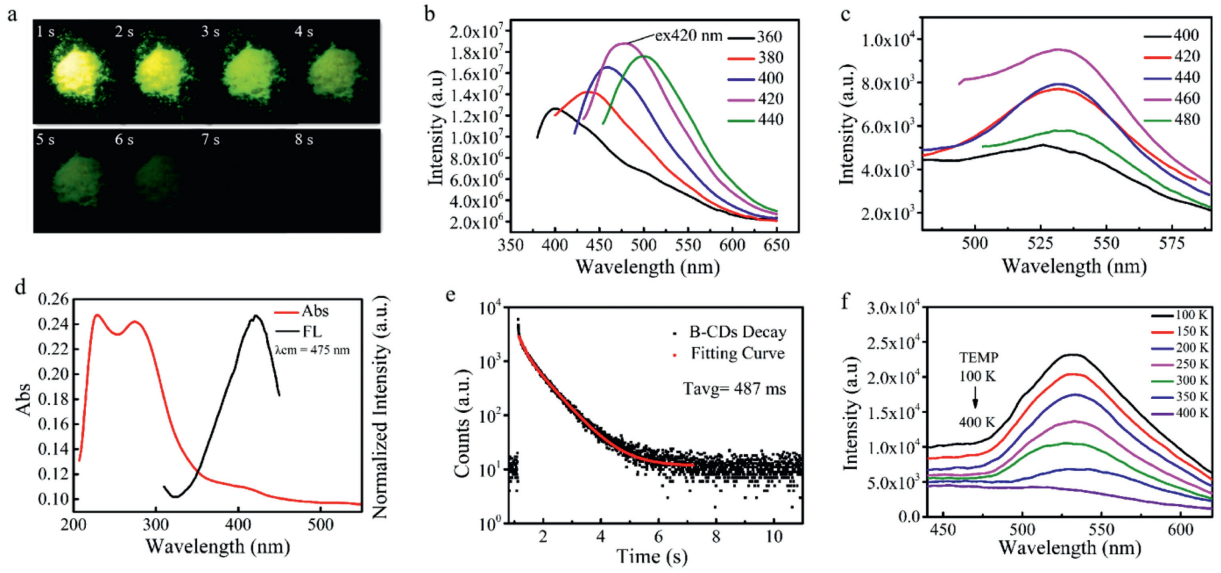

Fig. 2. (a) Photos of delayed afterglow of the B-CDs after UV lamp (365 nm) was turned off; (b) fluorescence and (c) phosphorescence emission spectra of the B-CDs material; (d) UV absorption and fluorescence excitation spectra of the B-CDs; (e) lifetime of the persistence emission at 530 nm of the B-CDs material excited by 365 nm UV light; (f) phosphorescence emission chart of B-CDs at various temperature from 100 K to 400 K. For interpretation of the references to color in this figure, the reader is referred to the web version of this article.

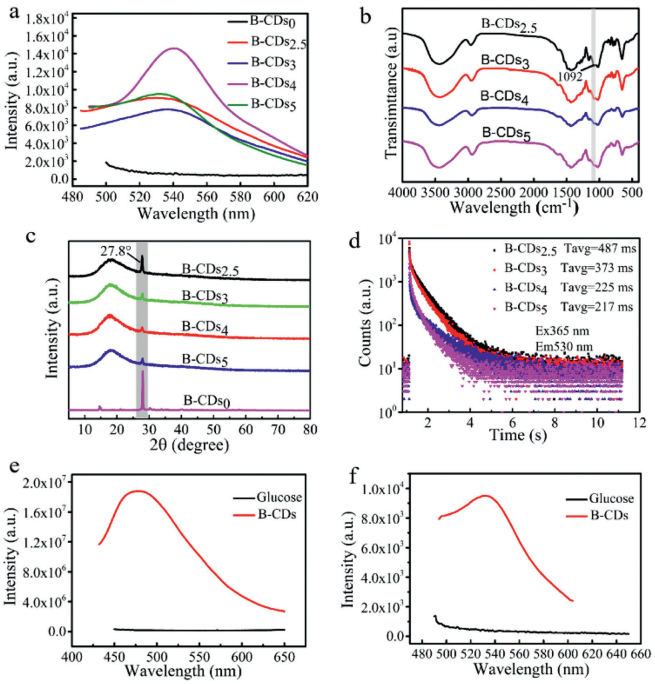

Fig. 3. (a) Phosphorescence emission spectra of B-CDs$_x$ (X = 0, 2.5, 3, 4, 5 g) excited at 460 nm. (b) FTIR spectrum of the B-CDs$_x$ (X = 2.5, 3, 4, 5 g); (c) the XRD analysis of the B-CDs$_x$ (X = 0, 2.5, 3, 4, 5 g); (d) Phosphorescence lifetime of B-CDs$_x$ (X = 2.5, 3, 4, 5 g), (e) FL emission spectra of glucose (black curve) and B-CDs (red curve); (f) Phosphorescence emission spectra of glucose (black curve) and B-CDs (red curve). For interpretation of the references to color in this figure legend, the reader is referred to the web version of this article.

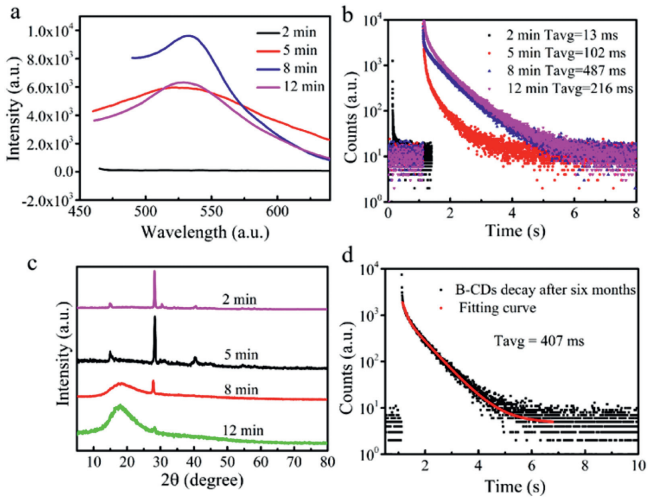

Fig. 4. (a) Phosphorescence emission spectra, (b) Phosphorescence lifetime and (c) XRD of microwave the B-CDs for 2, 5, 8, 12 min; (d) Phosphorescence lifetime of B-CDs after 6 months.

These findings have effectively proven that glucose and boric acid were chemically combined, and that the RTP of B-CDs was mainly due to the formation of B-C covalent bond between boric acid and glucose. The obvious characteristics of boron atoms in B-CDs revealed that they worked as the main body which produced covalent bonds with different strengths and crystalline characteristics depending on different proportions of glucose. These characteristics affected the performance of RTP.

To further explore the process of generating RTP from B-CDs, we conducted tests with various microwave time for 2, 5, 8, and 12 min to observe the RTP phenomenon. The sample did not show any phosphorescence of the sample after a two-minute treatment by microwave but exhibited the strongest phosphorescence with the longest lifetime when the sample was treated by microwave for eight minutes (Fig. 4a). In addition, the lifetime of the material had the longest lifetime when it was treated by microwave for 8 min while the lifetime was decreased when treated for 12 min (Fig. 4b). These results revealed that the most ideal processing time should be 8 min. The analysis of XRD suggested that the material only showed the characteristic peak of boron oxide when it was treated by microwave for 2 min (Fig. 4c). As the microwave time became longer, the lifetime of the material decreased, and the characteristic of the amorphous glass state was gradually obvious

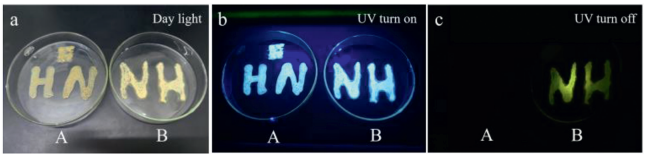

Fig. 5. Photographs of chitosan on the "A" Petri dish and chitosan and B-CDs mixture on the "B" Petri dish in (a) daylight, UV (b) on and (c) off (For interpretation of the references to color in this figure, the reader is referred to the web version of this article).

with the appearance of the typical characteristic peak of boron oxide at 27.8° (Fig. 4c). When the microwave time reached twelve minutes, the 27.8° peak weakened, and the lifetime was also reduced (Fig. 4c). This may be because the further carbonization of the carbon dots reduced the surface molecules and consumed the emissive species, thus affecting the RTP of B-CDs. These results further illustrated that the formation of the amorphous glass state and the crystal characteristics of boron oxide contribute to the generation of RTP.

Based on the above discussion, we tried to unravel the reason of the RTP performance of the B-CDs. According to the formula of $E = h/k * C/\lambda$, the ΔEst was calculated as 0.25, which is a small value for effective ISC. This valid ΔEst should also be resulted from the formation of the newly formed covalent bond and amorphous glass state. The newly formed covalent bond and amorphous glass state stabilized the emission of the triplet state and prevented the triplet exciton from being quenched. At the same time, the doping of boron atom has its specific property. Boron atoms had empty p orbitals that could attract π transitions to form p-π^* conjugated systems, reducing the minimum unoccupied orbital energy level of the system [47]. Therefore, the newly formed B-C bond effectively reduced ΔEst and promoted the ISC between S1 and T1.

In addition, we investigated the stability of the material. After the materials were stored in air for 6 months, its RTP could still be observed, and the lifetime was 407 ms (Fig. 4d). This result suggests that the structure of the material was stable, which is of great significance for the realization of the application of the material. In recent years, the potential applications of RTP materials have been continuously proposed by researchers [50,51]. Inspired by the RTP characteristics of B-CDs materials, we further explored their potential as anti-counterfeiting materials. Firstly, chitosan was dispersed in ethanol, and we wrote "HN" on the "A" petri dish using the mixture. Then, we mixed B-CDs with chitosan in ethanol and wrote "NH" on the "B" petri dish. The "HN" and "NH" showed no significant difference under sunlight and ultraviolet light (Figs. 5a and b). After turning off the UV lamp (365 nm), a yellow-green RTP appeared in the "B" petri dish where the B-CDs were located, and no phenomenon was observed in the "A" Petri dish (Fig. 5c). This provides an effective strategy for the potential application of RTP materials in information encryption protection.

In summary, we have successfully developed a microwave strategy to synthesize RTP CDs hetero-atomized with boron in a single step in only eight minutes. Compared with the previous high temperature and high-pressure method for preparing CDs, our strategy was cleaner, simpler and faster. After the synthesized RTP material was irradiated with UV light, the RTP of 8 s could be observed by naked eyes after the lamp was turned off, and the phosphorescence lifetime was 487 ms. We also discovered that the introduction of boron atoms allowed the newly formed materials to generate covalent bonds containing boron and new crystal characteristics. The formed B-C bonds and other covalent bonds promoted the ISC and the non-radiation transition of triplet states. The produced glass state helped to stabilize the triplet states of the B-CDs and made its non-radiation inactivated, thus exhibiting the characteristics of yellow green RTP. Thus, our convenient strategy is powerful for producing unique RTP of CDs materials, paving the way for industry to producing organic materials that have promising application in many purposes, *i.e.*, anti-counterfeiting and encryption.

Declaration of competing interest

The authors declare that they have no known competing financial interests or personal relationships that could have appeared to influence the work reported in this paper.

Acknowledgments

We are grateful for the financial support from the National Natural Science Foundation of China (No. 21801052), Hainan University start-up fund (No. KYQD(ZR)1852) and the construction program of research platform in Hainan University (No. ZY2019HN09).

Supplementary materials

Supplementary data associated with this article can be found, in the online version, at doi:10.1016/j.cclet.2021.05.046.

References

[1] H. Wang, L.Q. Meng, X.X. Shen, et al., Adv. Mater. 27 (2015) 4041–4047.
[2] L.X. Xiao, Z.J. Chen, B. Qu, et al., Adv. Mater. 23 (2011) 926–952.
[3] Y. You, Curr. Opin. Chem. Biol. 17 (2013) 699–707.
[4] A.C. Grimsdale, K.L. Chan, R.E. Martin, et al., Chem. Rev. 109 (2009) 897–1091.
[5] M.S. Kwon, D. Lee, S. Seo, et al., Angew. Chem. Int. Ed. 126 (2014) 11359–11363.
[6] Y. You, K. Huang, X. Liu, et al., Small 16 (2020) 1906733.
[7] H. Chen, X. Ma, S. Wu, H. Tian, Angew. Chem. Int. Ed. 126 (2014) 14373–14376.
[8] Z. Wang, T. Li, B. Ding, X. Ma, Chin. Chem. Lett. 31 (2020) 2929–2932.
[9] Q. Xiong, C. Xu, N. Jiao, et al., Chin. Chem. Lett. 30 (2019) 1387–1389.
[10] J. Wang, Z. Huang, X. Ma, H. Tian, Angew. Chem. Int. Ed. 59 (2020) 9928–9933.
[11] R. Gao, D.P. Yan, Chem. Sci. 8 (2017) 590–599.
[12] N. Song, Z. Zhang, P. Liu, et al., Adv. Funct. Mater. (2021) 2009924.
[13] R. Hu, Y. Zhang, Y. Zhao, et al., Chem. Eng. J. 392 (2020) 124807.
[14] J. L. L, J. Q. G, H. L, Chem. Eng. J. 406 (2021) 126008.
[15] R. Giménez, O. Crespo, B. Diosdado, et al., J. Mater. Chem. C 8 (2020) 6552–6557.
[16] J. Yang, Y.Y. Zhao, Y. Meng, et al., Chem. Eng. J. 387 (2020) 124067.
[17] X. Yang, D. Yan, Chem. Sci. 7 (2016) 4519–4526.
[18] D. Li, X. Yang, D. Yan, ACS Appl. Mater. Interfaces 10 (2018) 34377–34384.
[19] S.Y. Lim, W. Shen, Z.Q. Gao, Chem. Soc. Rev. 44 (2015) 362–381.
[20] X.Y. Xu, R. Ray, Y.L. Gu, et al., J. Am. Chem. Soc. 126 (2004) 12736–12737.
[21] C. Shen, J. Wang, Y. Cao, et al., J. Mater. Chem. C 3 (2015) 6668–6675.
[22] Q. Feng, Z.G. Xie, M. Zheng, Chem. Eng. J. (2020) 127647.
[23] K. Jiang, Y.H. Wang, C.Z. Cai, et al., Adv. Mater. 30 (2018) 1800783.
[24] S. Tao, S. Lu, Y. Geng, et al., Angew. Chem. Int. Ed. 57 (2018) 2393–2398.
[25] N. X, T. Song, H. Xiong, Chin. Chem. Lett. 32 (2021) 1953–1956.
[26] D. Yang, D. Qu, L. An, et al., Chin. Chem. Lett. 32 (2021) 2292–2296.
[27] D. Li, F. Lu, J. Wang, et al., J. Am. Chem. Soc. 140 (2018) 1916–1923.
[28] J. He, Y. He, Y. Chen, et al., Chem. Eng. J. 347 (2018) 505–513.
[29] J. Joseph, A. Anappara, ChemistrySelect 2 (2017) 4058–4062.
[30] B. Wang, Y. Mu, H. Zhang, et al., ACS Cent. Sci. 5 (2019) 349–356.
[31] Y. You, K. Huang, X. Liu, et al., Small 16 (2020) 1906733.
[32] Y.F. Gao, H.L. Zhang, Y. Jiao, et al., Chem. Mater. 31 (2019) 7979–7986.
[33] W. Li, W. Zhou, Z. Zhou, et al., Angew. Chem. Int. Ed. 58 (2019) 7278–7283.
[34] X. Dong, L. Wei, Y. Su, et al., J. Mater. Chem. C 3 (2015) 2798–2801.
[35] J. Tan, R. Zou, J. Zhang, et al., Nanoscale 8 (2016) 4742–4747.
[36] G. Qu, Y. Zhang, X. Ma, Chin. Chem. Lett. 30 (2019) 1809–1814.
[37] Q. Feng, Z. Xie, M. Zheng, Chem. Eng. J. (2020) 127647.
[38] K. Jiang, Y. Wang, X. Gao, et al., Angew. Chem. Int. Ed. 57 (2018) 6216–6220.
[39] P. Long, Y. Feng, C. Cao, et al., Adv. Funct. Mater. 28 (2018) 1800791.
[40] Q. Feng, Z. Xie, M. Zheng, Chem. Eng. J. (2020) 127647.
[41] J. Wang, X.Y. Lou, Y. Wang, et al., Macromol. Rapid Commun. (2021) 2100021.
[42] Z. Yuan, J. Wang, L. Chen, et al., CCS Chem. 2 (2020) 158–167.
[43] K. Jiang, S. Hu, Y. Wang, et al., Small 16 (2020) 2001909.
[44] K. Jiang, X. Gao, X. Feng, et al., Angew. Chem. Int. Ed. 59 (2020) 1263–1269.
[45] P. Long, Y. Feng, C. Cao, et al., Adv. Funct. Mater. 28 (2018) 1800791.
[46] S.Y. Tao, S.Y. Lu, Y. Geng, et al., Angew. Chem. Int. Ed. 57 (2018) 2393–2398.
[47] W. Li, W. Zhou, Z. Zhou, et al., Angew. Chem. Int. Ed. 58 (2019) 7278–7283.
[48] X. Gouin, P. Grange, L. Bois, et al., J. Alloy. Compd. 224 (1995) 22–28.
[49] L.F. Pang, Wu H, M.J. Fu, et al., Microchim. Acta 186 (2019) 708.
[50] Q.X. Xiong, C. Xu, N.M. Jiao, et al., Chin. Chem. Lett. 30 (2019) 1387–1389.
[51] G.H. Wang, Z.F. Wang, B.B. Ding, X. Ma, Chin. Chem. Lett. 32 (2021) 3039–3042.